OPEN

Long Non-coding RNA *NEAT1*, NOD-Like Receptor Family Protein 3 Inflammasome, and Acute Kidney Injury

Rui Xue,[1] *Wai Han Yiu*,[1] *Kam Wa Chan*,[1] *Sarah W.Y. Lok,*[1] *Yixin Zou,*[1] *Jingyuan Ma,*[1] *Hongyu Li*,[1] *Loretta Y.Y. Chan,*[1] *Xiao Ru Huang,*[2] *Kar Neng Lai,*[1] *Hui Yao Lan*,[2] *and Sydney C.W. Tang*[1]

Key Points

- Long non-coding RNA (lncRNA) nuclear-enriched abundant transcript 1 (*NEAT1*) was upregulated in human and murine AKI. It returned to baseline after recovery in humans. Its knockdown preserved kidney function in animals.
- *In vitro*, LPS upregulated *NEAT1* by TLR4/NF-κB signaling and caused its translocation into the cytoplasm where it activated nucleotide oligomerization domain-like receptor family protein 3 by binding receptor of activated protein C kinase 1.

Abstract

Background AKI is common in hospitalized patients and is associated with high mortality. Inflammation plays a key role in the pathophysiology of AKI. Long non-coding RNAs (lncRNAs) are increasingly recognized as regulators of the inflammatory and immune response, but its role in AKI remains unclear.

Methods We explored the role of lncRNA nuclear-enriched abundant transcript 1 (*NEAT1*) in (*1*) a cross-sectional and longitudinal cohort of AKI in humans, (*2*) three murine models of septic and aseptic AKI, and (*3*) cultured C1.1 mouse kidney tubular cells.

Results In humans, hospitalized patients with AKI ($N=66$) demonstrated significantly higher lncRNA *NEAT1* levels in urinary sediment cells and buffy coat versus control participants ($N=152$) from a primary care clinic; among six kidney transplant recipients, *NEAT1* levels were the highest immediately after transplant surgery, followed by a prompt decline to normal levels in parallel with recovery of kidney function. In mice with AKI induced by sepsis (by LPS injection or cecal ligation and puncture) and renal ischemia-reperfusion, kidney tubular *Neat1* was increased versus sham-operated mice. Knockdown of *Neat1* in the kidney using short hairpin RNA preserved kidney function and suppressed overexpression of the AKI biomarker neutrophil gelatinase-associated lipocalin, leukocyte infiltration, and both intrarenal and systemic inflammatory cytokines IL-6, CCL-2, and IL-1β. In LPS-treated C1.1 cells, *Neat1* was overexpressed by TLR4/NF-κB signaling and translocated from the cell nucleus into the cytoplasm where it promoted activation of nucleotide oligomerization domain-like receptor family protein 3 inflammasomes by binding with the scaffold protein receptor of activated protein C kinase 1. Silencing *Neat1* ameliorated LPS-induced cell inflammation, whereas its overexpression upregulated IL-6 and CCL-2 expression even without LPS stimulation.

Conclusions Our findings demonstrate a pathogenic role of *NEAT1* induction in human and mice during AKI with alleviation of kidney injury in three experimental models of septic and aseptic AKI after knockdown of *Neat1*. LPS/TLR4-induced *Neat1* overexpression in tubular epithelial cells increased the inflammatory response by binding with the scaffold protein, receptor of activated protein C kinase 1, to activate nucleotide oligomerization domain-like receptor family protein 3 inflammasomes.

JASN 35: 998–1015, 2024. doi: https://doi.org/10.1681/ASN.0000000000000362

Introduction

AKI is commonly observed in hospitalized patients and is a potentially fatal complication of critical illness, including coronavirus disease 2019.[1,2] Among hospitalized patients in the critical care setting, over 50% of patients with AKI are sepsis related with a high mortality.[3] AKI can cause

[1]Division of Nephrology, Department of Medicine, School of Clinical Medicine, The University of Hong Kong, Queen Mary Hospital, Hong Kong, China
[2]Department of Medicine and Therapeutics, Li Ka Shing Institute of Health Sciences, The Chinese University of Hong Kong, Hong Kong, China

Correspondence: Prof. Sydney C.W. Tang, email: scwtang@hku.hk

Received: June 8, 2023 **Accepted:** April 19, 2024
Published Online Ahead of Print: April 30, 2024

See related editorial, "Inflammasomes and Acute Kidney Injury," on pages 985–987.

permanent kidney damage with a high risk of subsequent CKD,[4,5] imposing a major burden on health care resources.[5] Early detection and treatment improves the outcome of AKI and is the current focus of management.[5] Inflammation plays a pivotal role in the multifactorial pathogenesis of AKI,[6] and delineating its underlying mechanisms will identify novel biomarkers and therapeutic targets to enhance clinical management.

Long non-coding RNAs (lncRNAs) are more than 200 nucleotides in length[7] and have emerged as important regulators of gene expression during disease development and progression.[8] LncRNA nuclear-enriched abundant transcript 1 (*NEAT1*), one of the most extensively studied lncRNAs, maintains the structural integrity of the paraspeckles, a specific type of nuclear body in the interchromatin space whose function remains poorly understood.[9,10] There is accumulating evidence that *NEAT1* exerts a critical role in the progression of several diseases, including those of the kidney.[9,11,12] Viral infection and other intracellular damage can increase the expression of *Neat1* to activate inflammasomes.[13] Nonetheless, the function of *Neat1* in the regulation of inflammasome activation during AKI remains largely unknown.

The nucleotide oligomerization domain-like receptor family protein 3 (NLRP3) inflammasome is a critical component of innate immunity that comprises a sensor molecule NLRP3, the adapter apoptosis-associated speck-like protein containing a caspase activation and recruitment domains (ASC), and the effector protease caspase-1.[14,15] It is capable of sensing cellular stress due to a wide variety of stimuli, including invading pathogens, toxins, endogenous danger signals, and metabolic dysfunction.[16] Dysregulation of NLRP3 inflammasome activation is associated with many inflammatory diseases.[17] Two sequential steps are required for activation of NLRP3 inflammasome: priming and activation. The key priming event is the TLR4/NF-κB signaling–mediated transcription of NLRP3, IL-1β, and IL-18, and the activation step is characterized by recruitment of ASCs to assemble the NLRP3 inflammasome complex with consequent cleavage of pro-caspase-1.[17,18] Cleaved caspase-1 induces maturation and secretion of proinflammatory cytokines and apoptosis.[19]

In this study, we hypothesize that *Neat1* participates in the pathogenesis of AKI. To this end, we examined the expression profile of *NEAT1* in a cross-sectional and longitudinal cohort of AKI in humans, explored the association of *Neat1* expression with kidney inflammation and injury using animal models of septic and aseptic AKI, and dissected the underlying mechanisms by which *Neat1* is involved in promoting NLRP3 inflammasome activation in LPS-stimulated tubular epithelial cells.

Methods

Clinical Specimens

The use of human specimens for this study was approved by the Research Ethics Committee/Institutional Review Board of the University of Hong Kong (HKU)/Hospital Authority Hong Kong West Cluster. All patients and control participants gave informed consent before collection of urine and blood samples. The clinical and research activities being reported are consistent with the Principles of the Declaration of Istanbul as outlined in the Declaration of Istanbul on Organ Trafficking and Transplant Tourism. Serum/plasma were separated from blood cells by centrifugation at 3000 rpm for 10 minutes and stored at −80°C for further analysis. Leukocytes from blood samples were prepared by removal of red blood cells from the buffy coat fraction using ammonium–chloride–potassium lysing buffer (Gibco, Grand Island, NY). Urine specimens were centrifuged at 3000 rpm for 10 minutes and urinary sediments obtained after discarding the supernatant. Relative *NEAT1* expression was measured by reverse transcription-quantitative PCR (RT-qPCR) in urine sediment and buffy coat of non-AKI and AKI participants.

Cell Culture and Stimulation

Mouse kidney tubular epithelial cells (C1.1) from Dr. Rudolf Wüthrich, Switzerland,[20] were cultured in Dulbecco's modified Eagle medium/nutrient mixture F12 (Gibco), supplemented with 100 IU/ml penicillin, 100 μg/ml streptomycin (Gibco), and 10% FBS (Invitrogen, Carlsbad, CA) at 37°C in 5% carbon dioxide atmosphere. Human embryonic kidney 293 cells (293T) (ATCC, Manassas, VA) were cultured in Dulbecco's modified Eagle medium with high glucose and GlutaMAX (Gibco), supplemented with 100 IU/ml penicillin, 100 μg/ml streptomycin, and 10% FBS at 37°C in 5% carbon dioxide atmosphere. For LPS priming, C1.1 cells were serum starved for 24 hours and stimulated with 200 ng/ml LPS (Sigma-Aldrich, St. Louis, MO). To inhibit TLR4 and NF-κB signaling, cells were pretreated with 5-μM CLI-095 (InvivoGen, San Diego, CA), 1-μM Bay11-7085, or 2.5-μM JSH-23 (Selleck Chemicals, Houston, TX) for 1 hour before LPS stimulation. For inflammasome activation, cells were primed with 1000 ng/ml LPS for 3 hours and stimulated with 5-μM nigericin (InvivoGen) for 1 hour.

Transfection

To knock down *Neat1*, C1.1 cells were transfected with antisense locked nucleic acid GapmeRs *Neat1* or negative control (QIAGEN, Germantown, MD) using the Lipofectamine 2000 reagent (Invitrogen). For double transfection using the X-tremeGENE small interfering RNA (siRNA) Transfection Reagent (Roche, Basel, Switzerland), cells were cotransfected with immediate early promoter of the human cytomegalovirus-*Rack1* or immediate early promoter of the human cytomegalovirus empty plasmids (OriGene, Rockville, MD) together with corresponding GapmerR or cotransfected with plasmid cloning DNA (pcDNA) 3.1-*Neat1* or empty plasmid (Invitrogen) and siRNA-*Rack1* or scrambled siRNA (Invitrogen).

In the co-immunoprecipitation experiment, 293T cells were transfected with pcDNA3-Flag-NLRP3 (Addgene 75127), pcDNA3-Flag-ASC plasmid (Addgene 75134) (a gift from Bruce Beutler), and siRNA *Neat1* or negative control (Invitrogen) using the Lipofectamine 2000 reagent.

Mouse Model and *Neat1* Knockdown

All animal experiments were approved by the Committee on the Use of Live Animals in Teaching and Research, HKU, and adhered to the National Institute of Health Guide for the Care and Use of Laboratory Animals. Male C57BL/6J mice weighing 20–25 g at 8 weeks of age were supplied by

the Centre for Comparative Medicine Research, HKU. To specifically knock down *Neat1* in the mouse kidney, small hairpin RNA-pSuper.puro vector targeting *Neat1* (200 μg/mouse) or pSuper.puro empty vector (OligoEngine, Seattle, WA) was mixed with Sonovue microbubbles (Bracco, Milan, Italy) in a ratio of 1:1 (vol:vol) and injected into mice through the tail vein. An ultrasound transducer (Therasonic, Electro Medical Supplies, Wantage, United Kingdom) was immediately applied on both kidneys with a pulse-wave output of 1 MHz at 2 W/cm^2 for 5 minutes on each side. The *Neat1* knockdown efficiency is shown in Supplemental Figure 1, A and B. Different models of AKI (LPS-, cecal ligation and puncture [CLP]-, and ischemia-reperfusion [IR]-induced) were established on experimental mice at day 3 after ultrasound-mediated gene transfer. In LPS-induced AKI, LPS (20 mg/kg), dissolved in 0.9% saline, was injected into mice by intraperitoneal injection. Saline was given to control animals. All animals were euthanized at 12 and 24 hours after LPS injection. In CLP-induced AKI, sepsis was induced by cecal ligation and puncture at 12 mm from the end of the cecum. Mice were resuscitated with saline injection (1 ml) and euthanized at 24 hours after CLP surgery. In IR-induced AKI, bilateral renal pedicles were clamped for 30 minutes with microaneurysm clips, followed by 24-hour reperfusion before sacrifice. All mice in the sham group underwent abdominal incision only. In all AKI models, kidneys were harvested after sacrifice, in which half were snap-frozen in liquid nitrogen and stored at −80°C. The other half were fixed with 10% formalin and embedded in paraffin.

RNA Extraction and Real-Time Quantitative PCR

Total RNAs from urinary sediments, leukocytes, and cultured cells were extracted by TRIZOL LS and TRIZOL reagent (Invitrogen) and that from kidney cortical tissues by the NucleoSpin RNA/Protein kit (Macherey-Nagel, Duren, Germany). RNAs were then reverse transcribed to cDNA using a High-Capacity cDNA Reverse Transcription Kit (Applied Biosystems, Carlsbad, CA). Real-time quantitative PCR was performed using SYBR Green reagent and specific primers on the StepOnePlus Real-Time PCR System (Applied Biosystems). Relative gene expression was obtained after normalization with glyceraldehyde-3-phosphate dehydrogenase (GAPDH), followed by comparison with the respective control group using StepOne software v2.3 (Applied Biosystems). The primer sequence of target genes is listed in Supplemental Table 1.

Western Blot Analysis

Total proteins were prepared from cultured cells using radioimmunoprecipitation assay (RIPA) lysis buffer (Millipore, Bedford, MA) with 10% Protease Inhibitor Cocktail (Sigma-Aldrich) and from kidney cortical tissue using the T-PER Tissue Protein Extraction Reagent (Thermo Scientific, Waltham, MA) and NucleoSpin RNA/

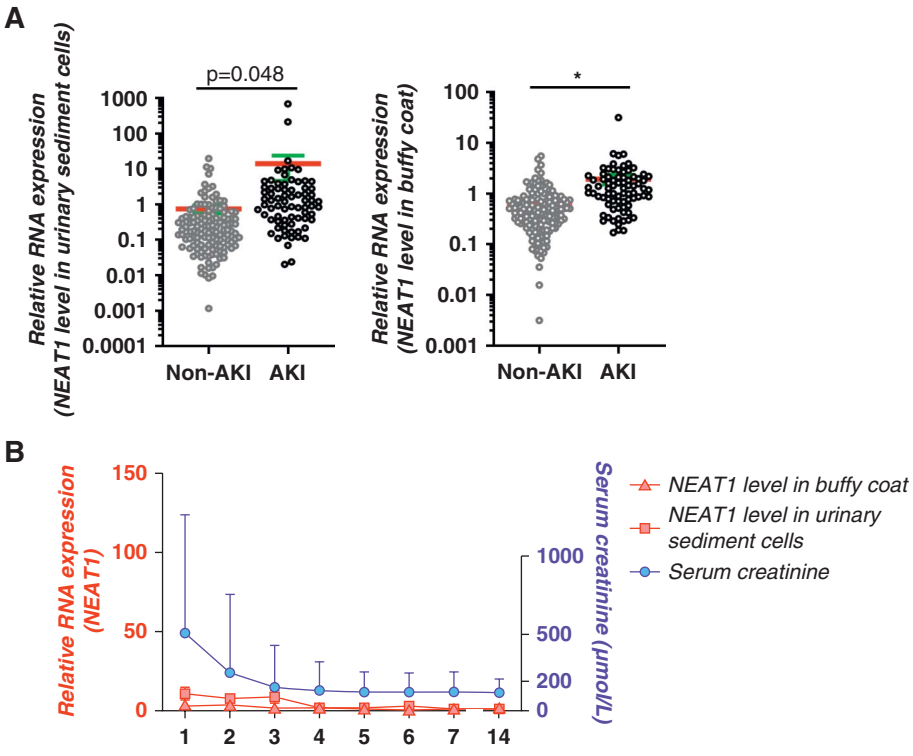

Figure 1. Changes of *NEAT1* levels in urinary sediment cells and buffy coat from patients with AKI. (A) Cross-sectional cohort among 66 hospitalized patients with AKI versus 152 control participants without AKI from a primary care clinic (data were presented in a logarithmic scale). (B) Longitudinal cohort (N=6) showing temporal changes in *NEAT1* levels in relation to kidney function after kidney transplantation. *$P < 0.001$. *NEAT1*, nuclear-enriched abundant transcript 1. Figure 1 can be viewed in color online at www.jasn.org.

Table 1. Demographics of participants

Characteristic	All Patients (*N*=218)	Non-AKI Participants (*N*=152)	AKI Participants (*N*=66)
Age, yr	70±9	67±4.3	76±13.9
Female ratio, no. (%)	97 (45)	72 (47)	25 (38)
Urine albumin-to-creatinine ratio, mg/mmol[a]	3±5	2±2	15±8
Urine sediment *Neat1* expression[a]	0.14±72	0.06±112	1.14±5
Buffy coat *NEAT1* expression[a]	0.52±4	0.37±4	1.21±2
Hemoglobin A1C, %	7±1	7±1	7±2
History of diabetes, yr	8±9	8±8	8±10
Smoking history, no. (%)			
Ex- or current smoker	41 (19)	24 (16)	17 (26)
Comorbidity, no. (%)[b]			
CKD	126 (58)	61 (40)	65 (99)
Any metabolic-related disorders	200 (92)	139 (92)	61 (92)
Diabetes	143 (66)	106 (70)	37 (56)
Hypertension	162 (74)	108 (71)	54 (82)
Dyslipidemia	151 (69)	110 (72)	41 (62)
Hyperuricemia	17 (8)	4 (3)	13 (20)
Cardiovascular disease	62 (28)	16 (11)	46 (70)
Any heart disease	49 (23)	10 (7)	39 (59)
Coronary artery disease	29 (13)	8 (5)	21 (32)
Congestive heart failure	18 (8)	1 (0.7)	17 (26)
Atrial fibrillation	24 (11)	2 (1)	22 (33)
Stroke/transient ischemic attack	16 (7)	5 (3)	11 (17)
Peripheral artery disease	8 (4)	2 (1)	6 (9)
Neoplasm	18 (8)	7 (5)	11 (17)

Demographics are presented in mean±SD. *NEAT1*, nuclear-enriched abundant transcript 1.
[a]Geometric mean.
[b]Does not add up to 100% because of co-presence of comorbidities.

Protein kit. Cytoplasmic and nuclear proteins were separated using an NE-PER Nuclear and Cytoplasmic Extraction kit (Thermo). Protein lysates were resolved by SDS-PAGE in Bolt 4%–12% gel (Invitrogen) and transferred to a polyvinylidene fluoride membrane (Millipore). Membranes were blotted with 5% nonfat milk and incubated with primary antibodies overnight at 4°C, followed by peroxidase-conjugated secondary antibodies (Dako, Carpinteria, CA) for 1 hour. Proteins were visualized with Clarity Western enhanced chemiluminescence Substrate (Bio-Rad, Hercules, CA) using the ChemiDoc XRS+ system (Bio-Rad). Relative expression of target protein was normalized with GAPDH expression using Image Lab 3.0 (Bio-Rad). Primary antibodies against p-p65 (3033) and p65 (8242) (Cell Signaling Technology, Beverly, MA); GAPDH (ASB16, Sigma-Aldrich); receptor of activated protein C kinase 1 (Rack1) (ab245401, Abcam, Cambridge, United Kingdom); CCL-2 (sc-52701) and IL-6 (sc-57315, Santa Cruz Biotechnology, Santa Cruz, CA); ASC (AG-25B-0006), pro-caspase-1, and cleaved caspase-1 (AG-20B-0044, AdipoGene Life Sciences, San Diego, CA); and NLRP3 (bs-10021R, Bioss Antibodies, Woburn, MA) were used.

Table 2. Clinical details of kidney transplant recipients (*N*=6)

Parameter	Recipients
Female ratio, no. (%)	2 (33)
Age at transplantation, yr	41±7
Causes of kidney failure	Nephrosclerosis (*n*=2) Reflux nephropathy (*n*=1) Alport syndrome (*n*=1) Dysplastic kidneys (*n*=1) Unknown (*n*=1)
Mode of dialysis before transplant, no. (%)	
PD	4 (67)[a]
Dialysis vintage, mo	26–85
Type of transplant, no. (%)	
Living donor	4 (67)
Cadaveric	2 (33)
No. of previous transplants, no. (%)	
None	5 (83)
One	1 (17)

PD, peritoneal dialysis.
[a]The remaining two patients underwent preemptive kidney transplant.

ELISA

The human serum level of IL-6 (D6050B) and IL-8 (DY208) was measured using a human ELISA kit (R&D Systems, Minneapolis, MN). The level of IL-6 (DY406) and CCL-2 (DY479) in supernatant from cultured cells and level of IL-6 (DY406), TNF-α (DY410), and IL-1β (DY401) from mouse serum were detected using a mouse ELISA kit (R&D Systems) according to the manufacturer's instructions.

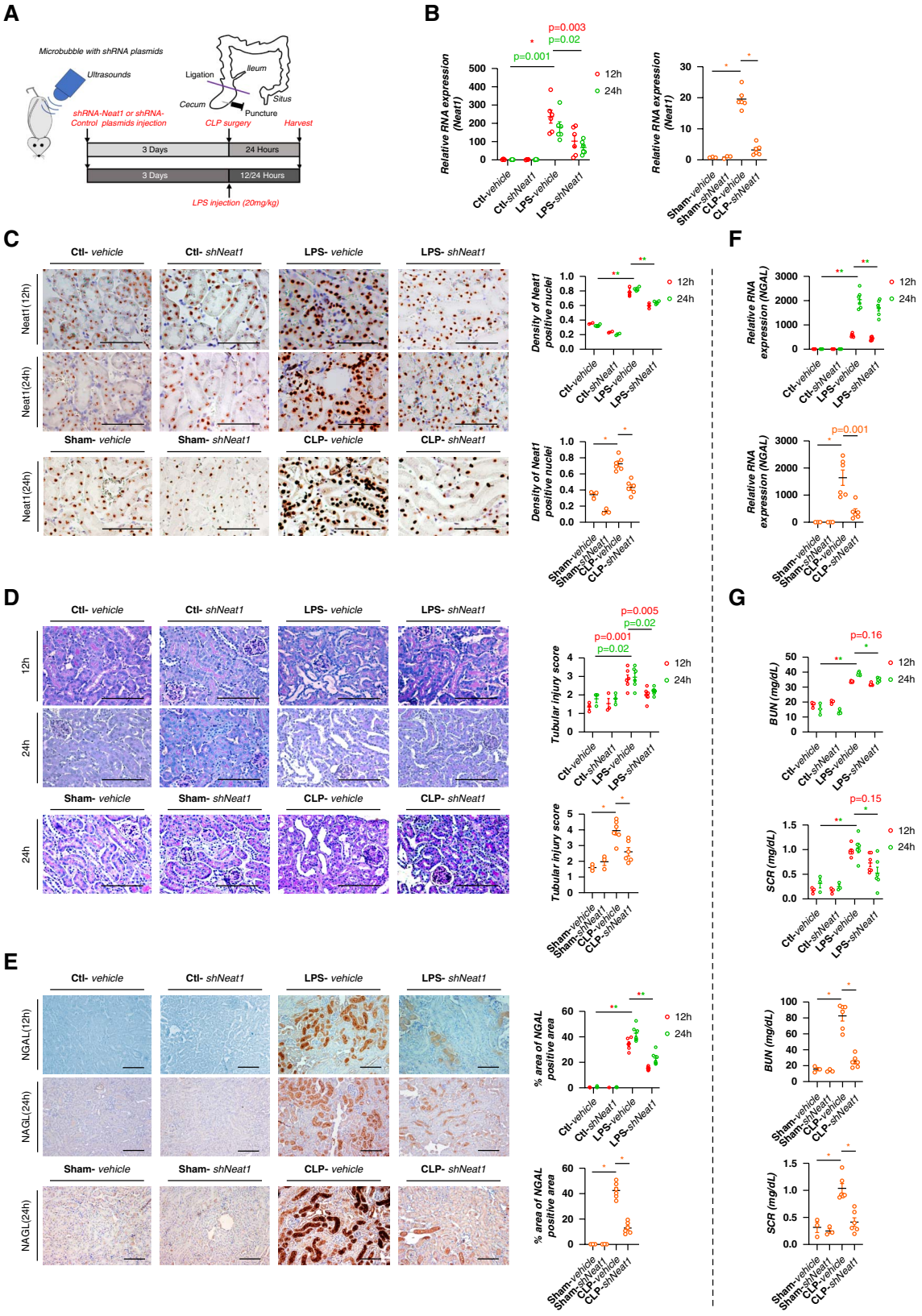

Figure 2. Knockdown of *Neat1* reduced AKI biomarkers and improved kidney function in sepsis-induced AKI mice. (A) Experimental design. Three days before LPS injection or CLP surgery, sh*Neat1* or empty plasmid (vehicle) was delivered into the kidney of C57BL/6J mice by tail vein injection, followed by ultrasound microbubble-mediated gene transfer. (B) Relative *Neat1* expression in the kidney at 12 and 24 hours after LPS injection and 24 hours after CLP surgery (Ctl, $n=3$; LPS, $n=6$; Sham, $n=3$; CLP, $n=6$). (C) Representative ISH

Figure 2. *Continued.* of *Neat1* expression in the kidney and the corresponding quantitative analyses (Ctl, $n \geq 2$; LPS, $n=4$; Sham, $n=3$; CLP, $n=6$). Scale bar=100 μm. (D) Representative kidney morphology and the corresponding quantitative analyses (Ctl, $n=3$; LPS, $n=6$; Sham, $n=3$; CLP, $n=6$). Scale bar=100 μm. (E) Representative immunohistochemical staining of NGAL and the corresponding quantitative analyses (Ctl, $n=3$; LPS, $n=6$; Sham, $n=3$; CLP, $n=6$). Scale bar=100 μm. (F) Relative mRNA expression of NGAL in the kidney (Ctl, $n=3$; LPS, $n=6$; Sham, $n=3$; CLP, $n=6$). (G) Measurement of serum BUN and serum creatinine levels by ELISA (Ctl, $n=3$; LPS, $n=6$; Sham, $n=3$; CLP, $n=6$). All data are expressed as mean±SEM, $^*P < 0.001$. CLP, cecal ligation and puncture; ctl, control; ISH, *in situ* hybridization; NGAL, neutrophil gelatinase–associated lipocalin; SCR, serum creatinine; sh*Neat1*, shRNA plasmid targeting *Neat1*; shRNA, small hairpin RNA.

Kidney Function Assessment

In humans, serum creatinine in AKI and control participants and kidney transplant recipients from day 1 to day 7 and day 14 was reported by service clinical biochemistry laboratories. In animals, serum creatinine and BUN were determined by the Creatinine LiquiColor Test (Stanbio Laboratory, Boerne, TX) and QuantiChrom Urea Assay Kit (BioAssay Systems, Hayward, CA), respectively, according to the manufacturer's instructions.

Histological Staining

Paraffin-embedded kidney tissue was sectioned (4-μm thickness), deparaffinized, rehydrated, and followed by a periodic acid-Schiff (Polysciences Inc., Warrington, PA) staining protocol. Tubular injury of the sections was scored according to the percentage of damaged renal tubules from 0 to 5: 0, normal; 1, tubular lesion <10%; 2, 10%–20% lesion; 3, 20%–30% lesion; 4, 30%–40% lesion; and 5, >40% lesion. Percentage of tubular injury of the medulla sections was scored according to the number of injured tubules.

Immunohistochemical Staining

After deparaffinization and rehydration, paraffin-embedded kidney sections were heated in citrate buffer (10 mM, pH 6.0) or protease K solution (10 μg/ml, pH 8.0) for antigen retrieval. Sections were quenched by 3% hydrogen peroxide and blocked with 2% BSA (Sigma-Aldrich). Primary antibodies against neutrophil gelatinase-associated lipocalin (ab70287, Abcam) and Ly6B.2 (MCA771GA, Bio-Rad) were applied on the sections for overnight incubation at 4°C, followed by peroxidase-conjugated second antibodies (Abcam). Sections were developed using 3,3′-diaminobenzidine substrate (Dako) and counterstained with hematoxylin (Dako) before mounting. Staining was quantified using Image J analysis software (National Institutes of Health, Bethesda, MD).

RNA *In Situ* Hybridization

To determine the expression and localization of *Neat1* in kidney tissue sections, RNA *in situ* hybridization was performed using the RNAscope 2.5 HD assay (Advanced Cell Diagnostics, Hayward, CA) following the manufacturer's protocol. In brief, deparaffinized sections were treated with protease K and hybridized with a horseradish peroxidase-labeled *Neat1* probe. The signal was developed by 3,3′-diaminobenzidine substrate, and nuclei were counterstained by hematoxylin. Quantification of positive staining was performed using Image J analysis software (National Institutes of Health).

ASC Oligomerization

After LPS priming and nigericin treatment, cells were washed with cold PBS and lysed with 0.5% Triton X-100 solution with protease inhibitor cocktail. Cell lysates were centrifuged and separated into supernatant (Triton-soluble) and pellet (Triton-insoluble). Triton-soluble fraction was used as input. The Triton-insoluble fraction was cross-linked with 2-mM disuccinimidyl suberate (Thermo Scientific) and boiled with SDS loading buffer (Bio-Rad) for Western blot analysis.

Formation of ASC Speck-Like Aggregates

Transfected cells seeded on the Nunc Lab-Tek II Chamber Slide (Thermo Scientific) were stimulated with LPS and nigericin. After that, cells were fixed in 4% paraformaldehyde, permeabilized with 0.25% Triton X-100, and blocked with 5% BSA. Cells were incubated with anti-ASC antibody (NBP1-78977, Novus Biologicals, Littleton, CO) overnight at 4°C, followed by Alexa Fluor 594–conjugated secondary antibody (Invitrogen) for 1 hour. Nuclei were contained with 4′,6-diamidino-2-phenylindole (Thermo Scientific). Fluorescence images of ASC aggregates were visualized under a fluorescence microscope.

Chromatin Immunoprecipitation

A SimpleChIP Enzymatic Chromatin IP Kit (Magnetic Beads) (Cell Signaling Technology) was used to perform chromatin immunoprecipitation. In brief, LPS-stimulated cells were cross-linked with 37% formaldehyde (Sigma-Aldrich), followed by nuclease digestion and sonication. The protein-bound chromatin fragments were immunoprecipitated using antibodies against p65 (8242), Histone H3 (4620), or normal IgG (2729) (Cell Signaling Technology). The eluted DNA was purified and detected by RT-qPCR analysis using specific primers listed in Supplemental Table 1.

RNA Pull-Down and Mass Spectrometry

An RNA pull-down Kit (BersinBio, Guangzhou, China) was used according to the manufacturer's instructions. LPS-primed cells were lysed by RIPA lysis buffer with 10% Protease Inhibitor Cocktail. Magnetic bead complex with biotinylated *Neat1* probe or negative control LacZ probe was added to protein lysates for incubation. The RNA-protein-bead complexes were washed, and proteins eluted in protein elution buffer and separated by SDS-PAGE, followed by Western blot analysis or subjected to mass spectrometry (Center for PanorOmic Sciences, HKU). The mass spectrometry proteomics data have been deposited to the ProteomeXchange Consortium (https://proteomecentral.proteomexchange.org)

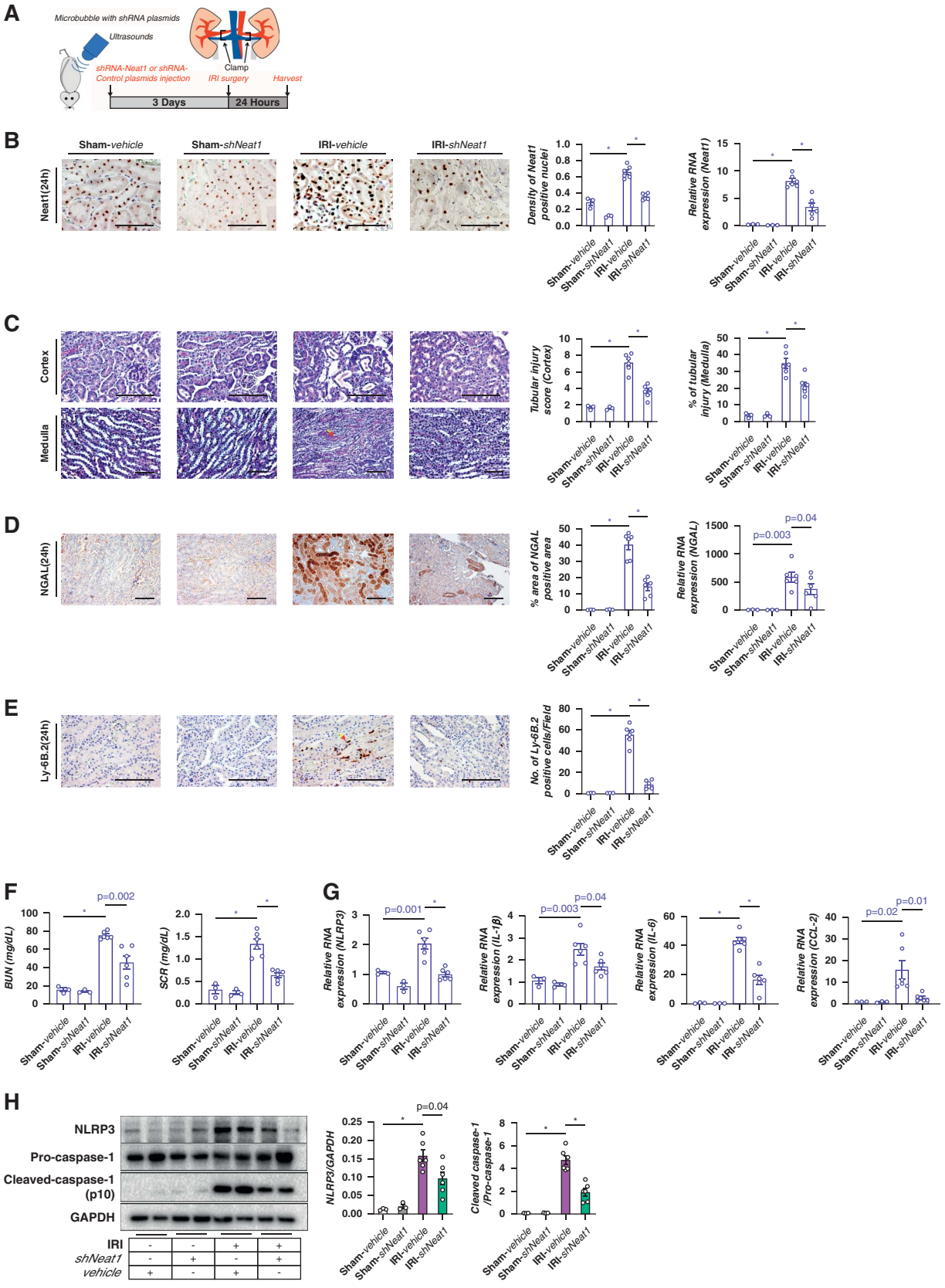

Figure 3. The renoprotective role of *Neat1* knockdown in IR-induced AKI mice. (A) Experimental design. Three days before IR surgery, shRNA plasmid targeting *Neat1* (sh*Neat1*) or empty plasmid (vehicle) was delivered into the kidney of C57BL/6J mice by tail vein injection, followed by ultrasound microbubble-mediated gene transfer. (B) Relative *Neat1* expression and representative ISH of *Neat1* expression with

Figure 3. *Continued.* the corresponding quantitative analyses in the kidney after IR surgery (Sham, $n=3$; IRI, $n=6$). (C) Representative morphology of the renal cortex and medulla (red arrowhead indicated injured areas) and the corresponding quantitative analyses (Sham, $n=3$; IRI, $n=6$). Scale bar=100 μm. (D) Representative immunohistochemical staining of NGAL with the corresponding quantitative analyses, and relative mRNA expression of NGAL in the kidney (Sham, $n=3$; IRI, $n=6$). Scale bar=100 μm. (E) Representative immunohistochemical staining of Ly6B.2 in the kidney interstitium (red arrowheads indicated positively stained cells) and the corresponding quantitative analyses (Sham, $n=3$; IRI, $n=6$). Scale bar=100 μm. (F) Measurement of serum BUN and serum creatinine levels by ELISA (Sham, $n=3$; IRI, $n=6$). (G) Relative mRNA expression of NLRP3, IL-1β, IL-6, and CCL-2 in the kidney (Sham, $n=3$; IRI, $n=6$). (H) Representative Western blot analyses of the expression levels of NLRP3, pro-caspase-1, and cleaved caspase-1 (p10) in the kidney after IR surgery, and the corresponding quantitative analyses (Sham, $n=3$; IRI, $n=6$). All data are expressed as mean±SEM, $^*P < 0.001$. GAPDH, glyceraldehyde-3-phosphate dehydrogenase; IR, ischemia-reperfusion; IRI, ischemia-reperfusion injury; NLRP3, NOD-like receptor family protein 3; NOD, nucleotide oligomerization domain.

using the iProX partner repository with the dataset identifier *PXD048489*.

RNA Immunoprecipitation

RNA immunoprecipitation (RIP) assay was performed using an EZ-Magna RIP (Cross-Linked) RNA-Binding Protein Immunoprecipitation Kit (Millipore) according to the manufacturer's instructions. In brief, cell lysate was prepared from LPS-primed cells and the protein-RNA complexes immunoprecipitated by incubation with Protein A/G magnetic beads (Santa Cruz Biotechnology) and anti-Rack1 antibody (ab245401, Abcam). Normal IgG was used as negative control (PP64B, Millipore). The immunoprecipitated RNAs were eluted and detected by RT-qPCR analysis. The results are presented as % Input Recovered. The primers used for detecting *Neat1* or U1 small nuclear RNA are listed in Supplemental Table 1.

Co-immunoprecipitation

293T cells transfected with pcDNA3-Flag-NLRP3, pcDNA3-Flag-ASC plasmids, siRNA-*Neat1*, and corresponding controls were stimulated with LPS/nigericin. The cells were lysed in RIPA lysis buffer with 10% Protease Inhibitor Cocktail and precleared with normal IgG (AG-35B-0013, AdipoGene) agarose beads. After centrifugation, the supernatants were incubated with anti-NLRP3 antibody (AG-20B-0006, AdipoGene) or normal IgG overnight at 4°C, followed by incubation with protein A/G agarose beads. Beads were washed with lysis buffer and boiled in SDS loading buffer with β-mercaptoethanol for Western blotting analysis.

Statistical Analyses

NEAT1 expression was log-transformed for statistical analysis. The association between AKI and *NEAT1* expression in urinary sediment cells and buffy coat was assessed by univariable and multivariable regression. In the multivariable analysis, age, sex, baseline eGFR, smoking history, and comorbidities (known diabetes, hypertension, dyslipidemia, hyperuricemia, coronary artery disease, congestive heart failure, atrial fibrillation, stroke/transient ischemic attack, peripheral artery disease neoplasm) were included into the regression model for adjustment. A sensitivity analysis was performed by recategorizing the comorbidities into CKD, metabolic-related disorders, cardiovascular disease, and neoplasms to account for collinearity of comorbidities. All intergroup comparisons are expressed as mean±SEM. Differences between experimental groups were evaluated by one-way ANOVA or t test using GraphPad Prism v.7 (GraphPad Software). $P < 0.05$ was considered statistically significant.

Results

NEAT1 Expression Was Higher in Patients with AKI

In the cross-sectional study, *NEAT1* levels in urinary sediment cells and buffy coat were significantly higher (Figure 1A) among 66 hospitalized patients with AKI (etiologies presented in Supplemental Table 2) versus 152 control participants without AKI recruited from a primary care clinic (Table 1). *NEAT1* levels in urinary sediment cells and buffy coat (fold change) in AKI and control participants were shown in Supplemental Figure 2, A and B. After adjusting for baseline eGFR, smoking history, and other comorbidities, AKI was associated with a 15.9- ($P = 0.006$) and 3.2- ($P < 0.001$) fold higher expression of *NEAT1* in the urine sediment and buffy coat, respectively (Supplemental Tables 3 and 4). The association remained robust in sensitivity analyses.

In the prospective longitudinal study of six patients with kidney failure (Table 2) who underwent kidney transplantation (and, therefore, deemed to have a scheduled ischemia-reperfusion AKI insult to the donor kidney), *NEAT1* levels in urinary sediment cells and buffy coat peaked immediately after transplant surgery and progressively declined to normal levels comparable with those observed among the non-AKI control participants stated above. The decline of *NEAT1* paralleled recovery of kidney function as reflected by decreasing serum creatinine (Figure 1B). Data for individual patients were shown in Supplemental Figure 2, C and D.

Neat1 Knockdown in Kidney Ameliorated Tubular Injury and Kidney Dysfunction in Sepsis- and IR-Induced AKI

To address the kidney-specific role of *Neat1* overexpression during AKI, mice with small hairpin RNA-mediated knockdown of *Neat1* (shRNA *Neat1*) (Figures 2A and 3A) were subjected to different animal models of AKI. LPS- and CLP-induced AKI models were used to mimic septic AKI, and ischemia-reperfusion injury was used to mimic aseptic AKI. *Neat1* gene expression was significantly increased in the kidney after LPS injection, CLP, and IR surgery, which was

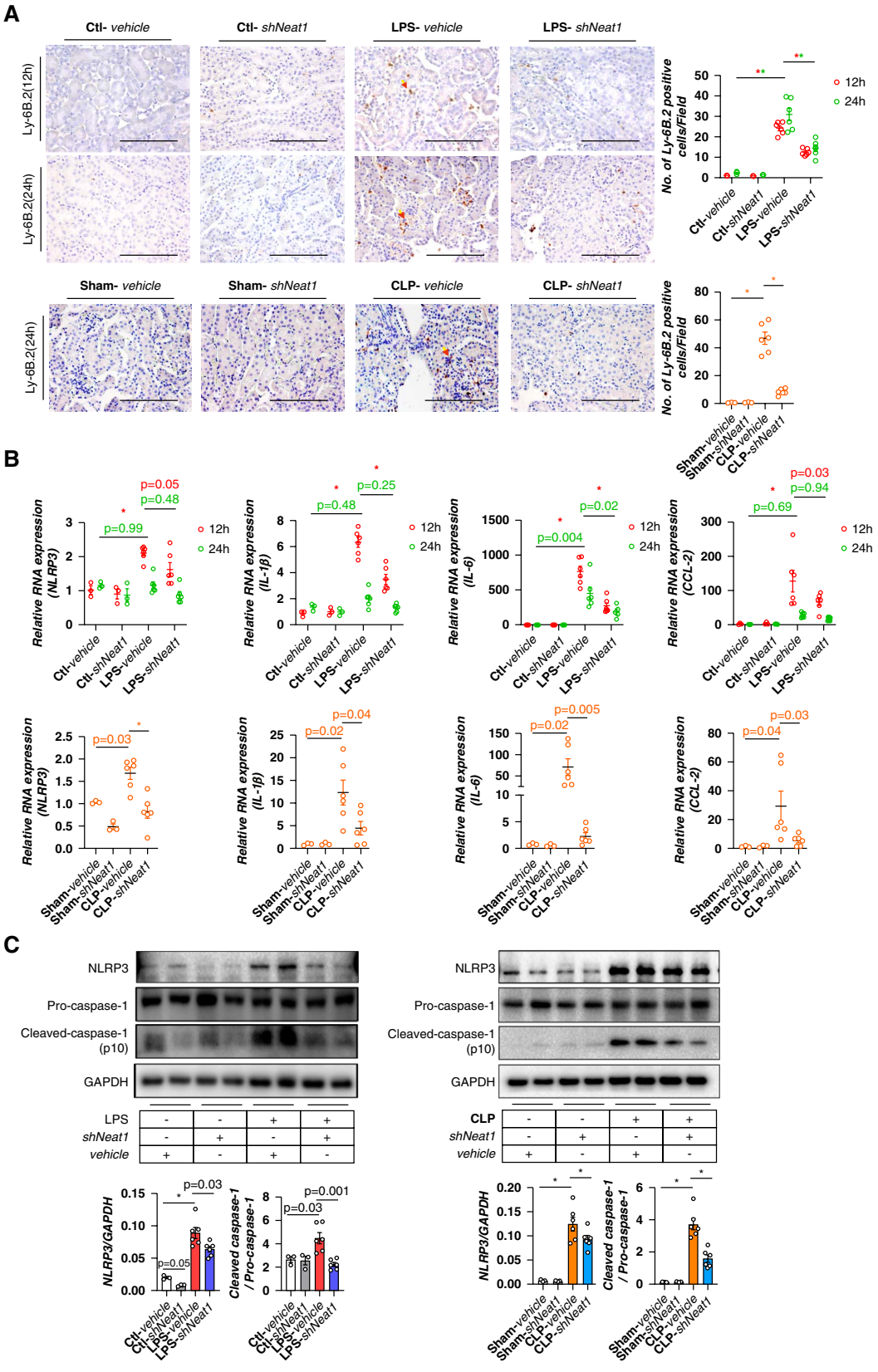

Figure 4. Knockdown of *Neat1* attenuated kidney inflammation by suppressing NLRP3 inflammasome activation in sepsis-induced AKI mice. (A) Representative immunohistochemical staining of Ly6B.2 in the kidney interstitium (red arrowheads indicated positively stained cells) and the corresponding quantitative analyses (Ctl, n=3; LPS, n=6; Sham, n=3; CLP, n=6). Scale bar=100 μm. (B) Relative mRNA expression

Figure 4. *Continued.* of NLRP3, IL-1β, IL-6, and CCL-2 in the kidney (Ctl, n=3; LPS, n=6; Sham, n=3; CLP, n=6). (C) Representative Western blot analyses of the expression levels of NLRP3, pro-caspase-1, and cleaved caspase-1 (p10) in the kidney at 12 hours after LPS injection and 24 hours after CLP surgery, and the corresponding quantitative analyses (Ctl, n=3; LPS, n=6; Sham, n=3; CLP, n=6). All data are expressed as mean±SEM, $^*P < 0.001$.

significantly attenuated after treatment with shRNA *Neat1* (Figures 2B and 3B). These findings were confirmed by RNA *in situ* hybridization that also demonstrated *Neat1*'s localization in tubular cell nuclei (Figures 2C and 3B). Morphologically, LPS and CLP surgery induced tubule dilation and brush border loss, which were ameliorated by shRNA *Neat1* in both septic AKI models (Figure 2D). In addition to cortical tubular injury, IR surgery induced tubular necrosis, cell detachment, and cast formation in the medulla, which were ameliorated by shRNA *Neat1* (Figure 3C). Kidney injury was profound in all AKI models as shown by overexpression of neutrophil gelatinase-associated lipocalin, which was significantly reduced by *Neat1* knockdown (Figures 2, E and F, and 3D). Biochemically, *Neat1* knockdown improved kidney function by reducing increases in BUN and serum creatinine in all three AKI models (Figures 2G and 3F).

Neat1 Induction Caused Kidney Inflammation and NLRP3 Inflammasome Activation in Sepsis- and IR-Induced AKI

Kidneys from LPS-, CLP-, and IR-induced AKI mice showed increased kidney interstitial expression of Ly-6B.2 and F4/80, whereas shRNA *Neat1*-treated mouse kidneys had attenuated neutrophil and macrophage infiltration (Figures 3E and 4A and Supplemental Figure 4A). *Neat1* knockdown also significantly reduced AKI-induced overexpression of NLRP3, IL-1β, IL-6, and CCL-2 in kidney tissue (Figures 3G and 4B). Circulating proinflammatory cytokine expression was shown in Supplemental Figure 3. Activation of intrarenal NLRP3 inflammasome was further demonstrated after LPS treatment, CLP, and IR surgery by upregulated NLRP3 protein levels in renal tubular cells and superinduction of cleaved caspase-1 in kidney tissue, which were all reversed by knockdown of *Neat1* (Figures 3H and 4C and Supplemental Figure 4B).

Neat1 Mediated TLR4/NF-κB–Regulated Inflammatory Responses in Both LPS- and Hypoxia/Reoxygenation-Stimulated Tubular Epithelial Cells

In cultured C1.1 tubular cells, LPS upregulated *Neat1* expression maximally at 60 minutes, which preceded that of proinflammatory cytokines CCL-2 and IL-6 at 90 and 120 minutes, respectively (Figure 5A). Transfection with antisense locked nucleic acid GapmeRs in C1.1 cells knocked down *Neat1* by 47% (Figure 5B), which significantly suppressed LPS-induced IL-6 overexpression at both gene (Figure 5C) and protein levels (Figure 5, D and E). Conversely, cells overexpressing *Neat1* after transfection with a pcDNA3.1-*Neat1* plasmid (Figure 5F) exaggerated expression of IL-6 and CCL-2 (Figure 5, G and H) versus control. In addition, *Neat1* expression was markedly increased under hypoxia-reoxygenation treatment, whereas knockdown of *Neat1* significantly reduced hypoxia-reoxygenation–induced inflammatory cytokine (IL-6 and CCL-2) production in C1.1 tubular cells (Supplemental Figure 5).

To unravel the mechanisms of *Neat1* expression, we used Integrative Genomics Viewer software and the online database AnimalTFDB 3.0 (http://bioinfo.life.hust.edu.cn/AnimalTFDB/#!/) and predicted four putative NF-κB binding sites on the promoter region of *Neat1* (Figure 6A). Chromatin immunoprecipitation-quantitative PCR demonstrated enrichment of p65 to the *Neat1* promoter (Figure 6B), suggesting that *Neat1* transcription may be regulated by TLR4/NF-κB signaling. This was confirmed by prevention of LPS-induced *Neat1* overexpression in C1.1 cells that were pretreated with the TLR4 inhibitor CLI-095 or NF-κB inhibitors (BAY11-7085, JSH-23) (Figure 6C). However, knockdown of *Neat1* did not affect p65 phosphorylation in LPS/nigericin-treated C1.1 cells (Figure 6D).

Silencing of *Neat1* Blocked NLRP3 Inflammasome Activation in LPS-Stimulated Tubular Epithelial Cells

To further investigate whether *Neat1* could promote NLRP3 inflammasome activation, C1.1 cells were transfected with different plasmids and stimulated with the following treatments: (*1*) GapmeRs control, (*2*) GapmeRs control with LPS, (*3*) GapmeRs control with LPS and nigericin, (*4*) GapmeRs *Neat1*, (*5*) GapmeRs *Neat1* with LPS, and (*6*) GapmeRs *Neat1* with LPS and nigericin. Silencing of *Neat1* in LPS-primed C1.1 cells prevented nigericin, an activator NLRP3 inflammasome, from resulting in pro-caspase-1 cleavage (Figure 6E). In addition, it also prevented the oligomerization of ASC despite concomitant stimulation with LPS and nigericin (Figure 6F). Similarly, ASC speck formation was also significantly suppressed under the same inflammasome stimulatory conditions (Figure 6G).

Neat1 Interacts with Rack1 and Regulates NLRP3 Inflammasome

There is growing evidence that lncRNAs regulate biological and pathological processes through direct interaction with proteins. To identify potential binding partners for *Neat1*, we performed a biotinylated *Neat1* 1 RNA pull-down assay followed by mass spectrometry in cell lysates from unstimulated and LPS-stimulated C1.1 cells. The protein-RNA complexes enriched by *Neat1* pull-down were silver-stained on SDS-PAGE (Supplemental Figure 6A) and subjected to mass spectrometry. Potential *Neat1* binding proteins were identified in LPS-stimulated cells compared with unstimulated control (Supplemental Figure 6B). Among them, Rack1 was selected for further validation of its functional role in NLRP3 inflammasome activation. Western blot analysis confirmed that Rack1 interacted with the biotinylated *Neat1* probe in the LPS-stimulated pull-down sample, but not with the non-specific LacZ probe (Figure 7A). The specific interaction between *Neat1* and Rack1 was further validated by the RIP assay (Figure 7B).

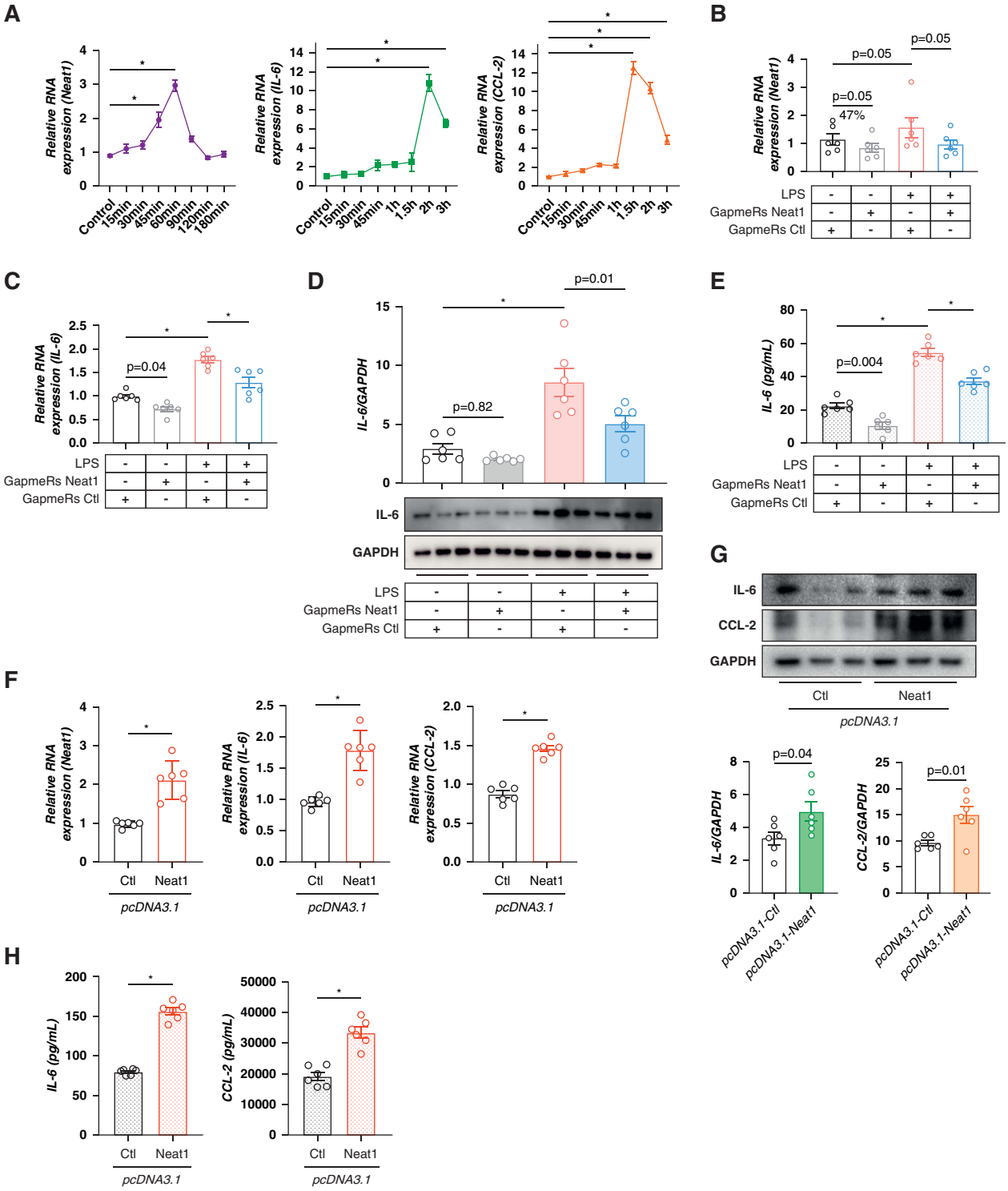

Figure 5. *Neat1* mediated inflammation in C1.1 mouse tubular cells. (A) Relative expression of *Neat1*, IL-6, and CCL-2 at different times after LPS stimulation by RT-qPCR (n=6). (B) Efficiency of *Neat1* knockdown by *Neat1* antisense locked nucleic acid GapmeR compared with negative control (Ctl) with or without LPS stimulation by RT-qPCR (n=6). Relative expression of IL-6 in cells transfected with Ctl or GapmeRs *Neat1* under LPS stimulation as determined by (C) RT-qPCR, (D) Western blotting, and (E) ELISA (n=6). (F) *Neat1* overexpression after transfection with pcDNA3.1 *Neat1* plasmids by RT-qPCR ($n \geq 6$). Relative expression of IL-6 and CCL-2 in cells transfected with Ctl or *Neat1* plasmids as determined by (F) RT-qPCR, (G) Western blotting, and (H) ELISA (n=6). All data are expressed as mean±SEM, $^*P < 0.001$. pcDNA, plasmid cloning DNA; RT-qPCR, reverse transcription-quantitative PCR. Figure 5 can be viewed in color online at www.jasn.org.

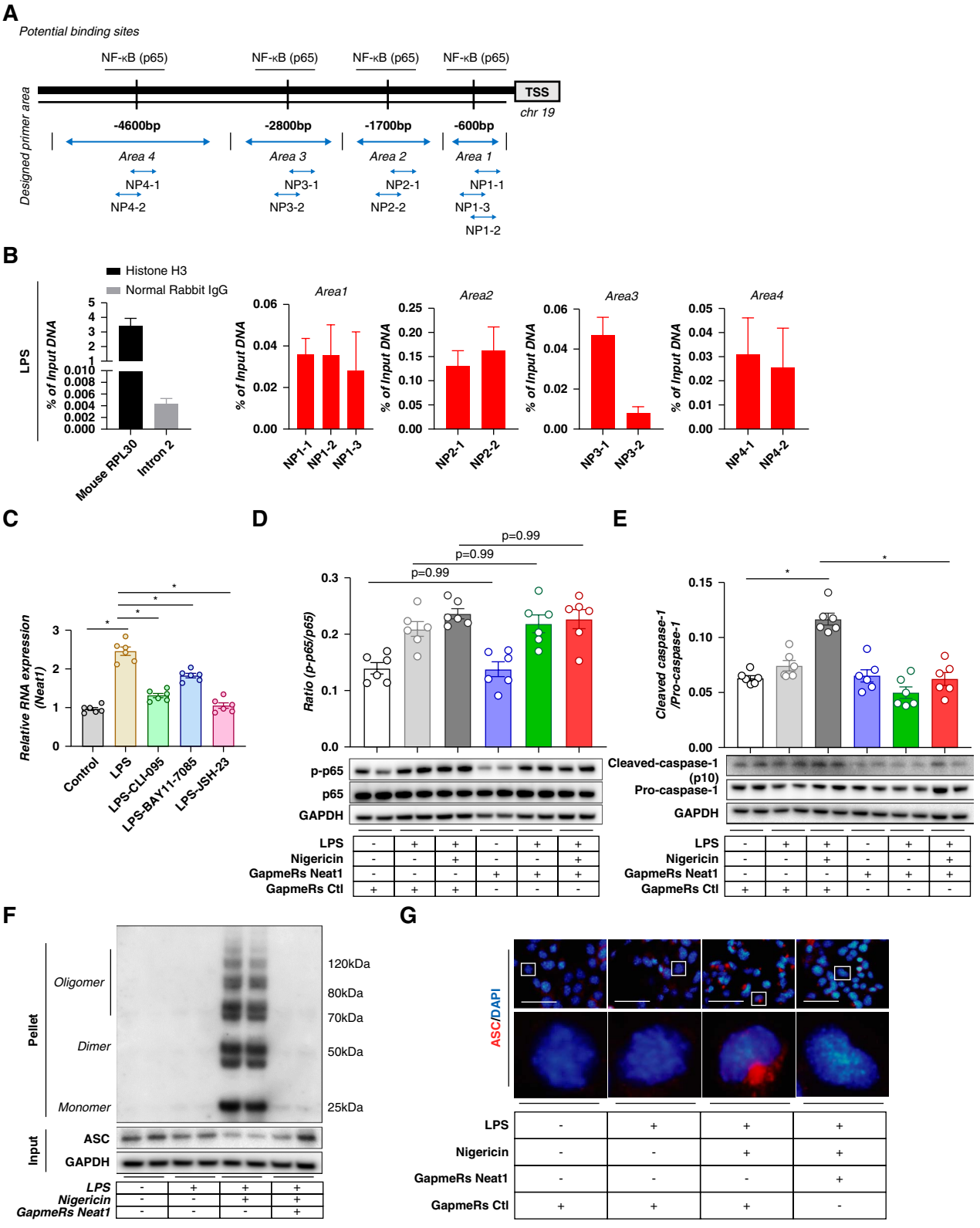

Figure 6. *Neat1*-mediated TLR4/NF-κB-induced NLRP3 inflammasome activation in C1.1 cells. (A) Schematic diagram of *Neat1*'s promoter region on mouse chromosome 19. Primers were designed for the four putative p65/NF-κB binding sites (areas 1–4). (B) Enrichment of the p65/NF-κB binding fragment presented as percentage relative to input DNA. Anti-histone H3 antibody and normal rabbit IgG were used as positive and negative controls, respectively (n=3). (C) Relative expression of *Neat1* under LPS stimulation with pretreatment of TLR4 inhibitor (CLI-095) or NF-κB inhibitors (BAY11-7085, JSH-23) by RT-qPCR (n≥5). (D) Representative Western blot analysis of expression levels of phospho-p65 and p65 in LPS-primed, nigericin-induced cells with Ctl or GapmeR *Neat1* and the corresponding quantitative analyses (n=6).

Figure 6. *Continued.* (E) Representative Western blot analysis of expression levels of pro-caspase-1 and cleaved caspase-1 (p10) in LPS-primed, nigericin-induced cells with Ctl or GapmeR *Neat1* and the corresponding quantitative analyses ($n \geq 5$). (F) Western blotting showing the effect of *Neat1* knockdown on ASC oligomerization in cell pellets from LPS-primed, nigericin-induced cells. Soluble cell lysates were used as input. (G) Representative immunofluorescence staining of endogenous ASC speck (red) and DAPI (blue) in LPS-primed, nigericin-induced cells with Ctl or GapmeR *Neat1*. Scale bar=50 μm. All data are expressed as mean±SEM, $^*P < 0.001$. ASC, apoptosis-associated speck-like protein containing a CARD; CARD, caspase activation and recruitment domains; DAPI, 4′,6-diamidino-2-phenylindole.

Rack1 serves as a scaffold protein and facilitates many biological processes; however, whether it interacts with *Neat1* during the activation of NLRP3 inflammasome remains unknown. In human embryonic kidney 293T cells cotransfected with pcDNA3-Flag-NLRP3 and pcDNA3-Flag-ASC plasmids, the co-immunoprecipitation assay revealed NLRP3-ASC-Rack1 interactions in LPS-primed, nigericin-treated cells. Gene silencing of *Neat1* disrupted these protein–protein interactions of the inflammasome complex (Figure 7C). The role of *Neat1* in Rack1-mediated NLRP3 inflammasome activation was further investigated by knocking down *Neat1* in C1.1 cells overexpressing Rack1. Under LPS/nigericin stimulation, both NLRP3 and cleaved caspase-1 expression were induced but significantly decreased after *Neat1* knockdown. Overexpression of Rack1 could not accentuate NLRP3 inflammasome activation or rescue the inactivation of NLRP3 inflammasome consequent to *Neat1* deficiency (Figure 7D). On the contrary, cells with *Neat1* overexpression further enhanced LPS/nigericin-induced NLRP3 expression and cleavage of caspase-1. The inflammasome activation was blunted by Rack1 knockdown although NLRP3 levels remained unchanged (Figure 7E). Expression of ASC remained unchanged (Figure 7, D and E) during these transfection experiments regardless of the transfection strategy or efficiency (Supplemental Figure 6, C and D). Altogether, our results suggest that *Neat1* promoted the expression of NLRP3 inflammasome and its assembly, leading to cleavage of pro-caspase-1.

Discussion

Since its discovery, *NEAT1* has been widely investigated in various human malignancies, including lung, colorectal, and prostate cancers, for its regulatory role in growth, proliferation, and apoptosis.[21–23] Until recently, *NEAT1* was recognized as an important immunomodulator in other diseases, such as liver disease,[24] rheumatoid arthritis,[25] and heart disease,[26] but its role in kidney disease has remained incompletely defined. We provide three lines of solid evidence that highlights a key role of *Neat1* in AKI. First, our human studies from a cross-sectional cohort indicated that *NEAT1* was overexpressed during AKI, which led to a >15-fold and >3-fold higher level in urinary sediment cells and buffy coat, respectively, after adjusting for baseline eGFR and comorbidities. We then made use of the fact that kidney transplantation is one form of planned AKI from surgical ischemia-reperfusion injury and demonstrated a temporal relation between the decline of heightened postoperative *NEAT1* in urine and blood to non-AKI levels and recovery of allograft kidney function after surgery.

Second, we adopted three mouse models to mimic the abovementioned clinical scenarios. Because sepsis was the most common cause of AKI in our cohort and other studies,[3,5] two septic AKI models were used, namely endotoxemia from LPS treatment and CLP-induced polymicrobial peritonitis. In addition, IR-induced AKI recapitulates aseptic AKI. Indeed, AKI is recognized as a systemic disease that not only leads to kidney lesions but also affects the immune system.[27] Our findings showed that mice with AKI due to either sepsis or ischemia-reperfusion injury exhibited systemic inflammatory responses, including increased leukocyte infiltration, tubular injury, and kidney failure. Third, LPS stimulated overexpression of *Neat1* in cultured C1.1 tubular cells. This is a particularly important observation as AKI is usually caused by acute tubular necrosis, leading to a rapid decline in kidney function.[5,28] Hence, our *in vitro* studies focused on tubular cells in which we showed for the first time that *Neat1* expression is regulated by TLR4/NF-κB signaling and that it interacted with the protein Rack1 to activate NLRP3 inflammasome.

As key regulators of immune responses, lncRNAs are involved in the production of inflammatory mediators, cell differentiation, and migration. *Neat1* is a ubiquitously expressed lncRNA that is enriched in the nucleus for paraspeckle formation. We identified *Neat1* as a downstream target of TLR4/NF-κB signaling, a major receptor-mediated pathway evoked by LPS.[29] TLR4/NF-κB signaling regulates various processes of the immune response by transcription of inflammatory genes.[30] Using loss- and gain-of-function approaches, we testified *Neat1*'s proinflammatory role because its deficiency prevented LPS-induced overexpression of IL-6/CCL2, whereas its overexpression increased these cytokines even without LPS stimulation. Such finding corroborated our animal data in which *Neat1* mediated IL-6 expression in mice with LPS-induced AKI, in agreement with our previous observation that NF-κB mediates TLR4-induced IL-6 expression in tubular cells.[31] Hence, reduction of proinflammatory cytokines produced by tubular cells with *Neat1* knockdown decreased immune cell infiltration that not only ameliorated kidney injury but improved the systemic inflammation by paracrine signaling. The involvement of *Neat1* in TLR4/NF-κB signaling has been reported in pyroptosis, apoptosis, and tumorigenesis,[32–34] but whether NF-κB activation is involved in *Neat1*-regulated inflammatory responses remains unknown. We observed that the p65, subunit of NF-κB directly bound to the promoter region of *Neat1* and that LPS-induced *Neat1* expression was suppressed by blocking TLR4/NF-κB signaling, suggesting a p65-mediated *Neat1* transcription. Collectively in our study, we detected LPS-induced *Neat1* expression as early as 45 minutes after LPS stimulation in mouse tubular C1.1

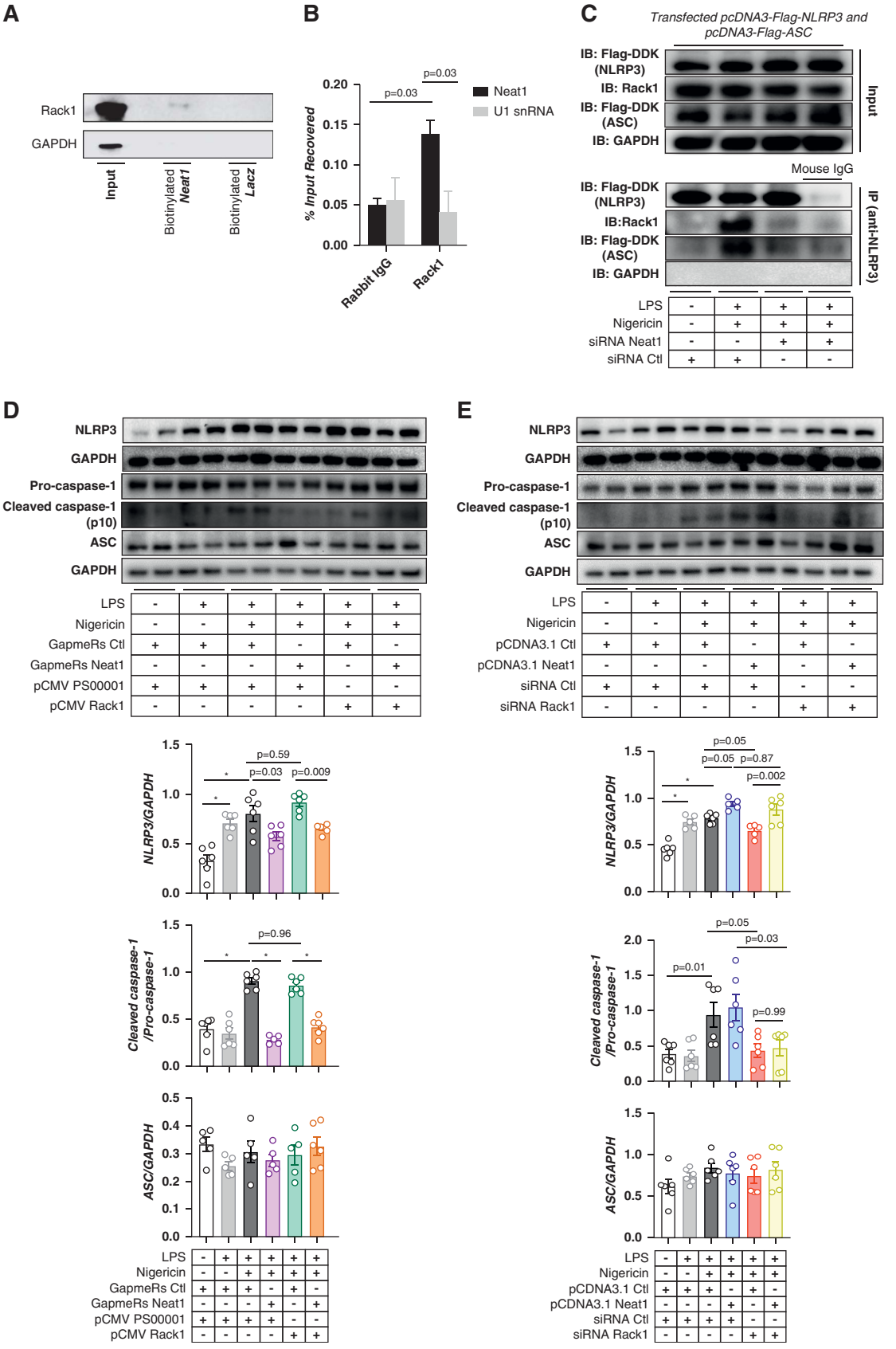

Figure 7. *Neat1* interacts with Rack1 and regulates NLRP3 inflammasome. (A) Detection of Rack1 by Western blotting in RNA pull-down sample using a biotinylated *Neat1* probe in LPS-stimulated C1.1 cells. The LacZ probe was used as negative control (n=3). (B) RIP using antibody against Rack1 or normal rabbit IgG (negative control) in LPS-stimulated C1.1 cell extracts followed by RT-qPCR with specific

Figure 7. *Continued.* primers to *Neat1* or U1 snRNA (negative control) ($n=3$). (C) Co-immunoprecipitation with anti-NLRP3 antibody on LPS-primed, nigericin-induced HK293T cells cotransfected with pcDNA3-Flag-NLRP3 and pcDNA3-Flag-ASC plasmids with control (Ctl) or *Neat1* siRNA. Normal mouse IgG was used as negative control ($n=3$). (D) Representative Western blot analysis of the effect of *Neat1* knockdown and Rack1 overexpression and (E) of the effect of *Neat1* overexpression and Rack1 knockdown on expression of NLRP3, pro-caspase-1, cleaved caspase-1 (p10) and ASC in LPS-primed, nigericin-induced C1.1 cells and quantification ($n\geq5$). All data are expressed as mean±SEM, $^*P < 0.001$. pCMV, immediate early promoter of the human cytomegalovirus; Rack1, receptor of activated protein C kinase 1; RIP, RNA immunoprecipitation; siRNA, small interfering RNA; snRNA, small nuclear RNA. Figure 7 can be viewed in color online at www.jasn.org.

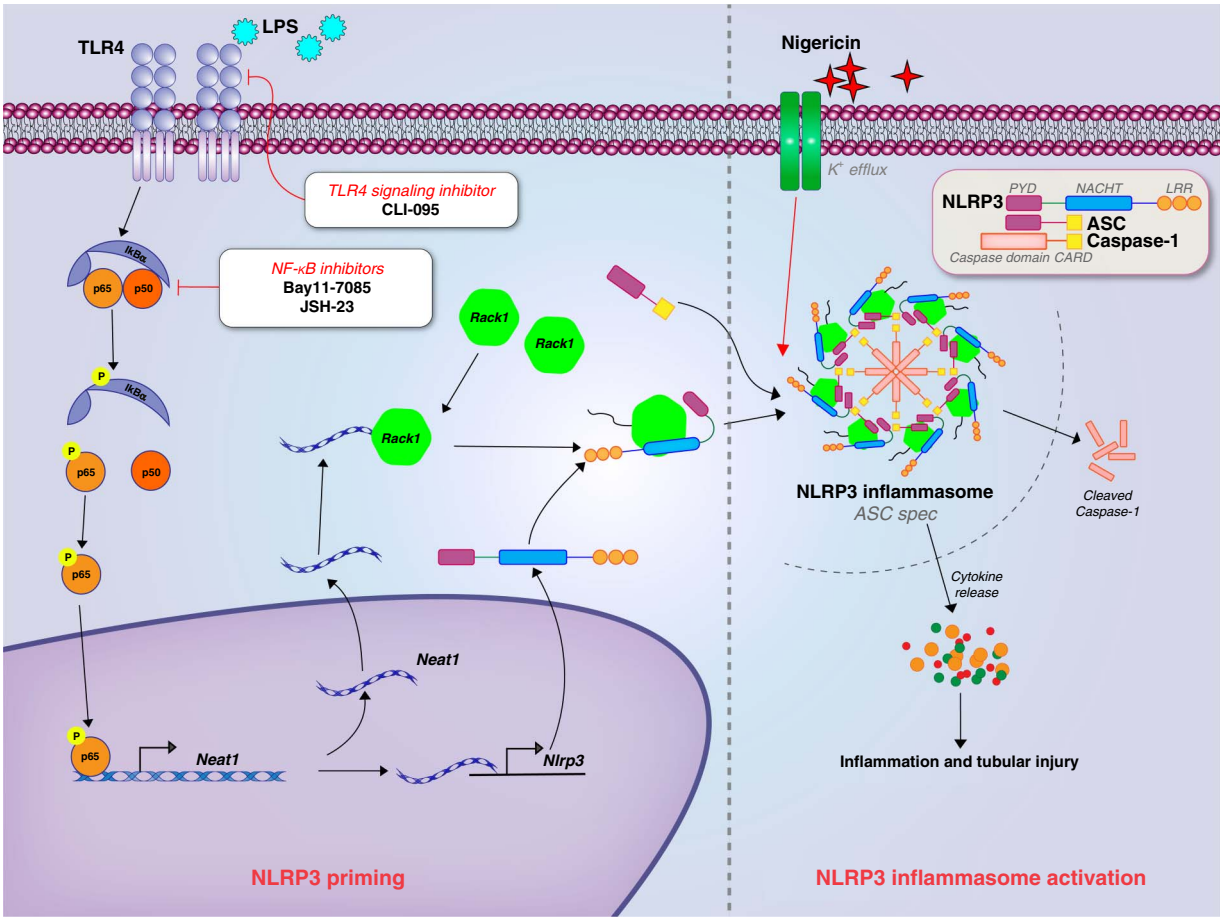

Figure 8. Schematic diagram showing *Neat1*'s role in NLRP3 inflammasome assembly triggered by LPS/nigericin.

cells (Figure 5A), but knockdown of *Neat1* did not affect LPS-induced NF-κB signaling responses, which was different from the case found in the study by Zhou *et al.*,[35] in which silencing of *NEAT1* inhibited p65 expression in LPS-induced human HK-2 cells. The discrepancy may be explained by the fact that different experimental conditions were used. In the study by Zhou *et al.*, cells were stimulated with 10 μg/ml LPS for 12 hours while only 1 μg/ml LPS was used for 4-hour stimulation in Figure 6D. In our case, the use of short-term LPS stimulation was due to the acute upregulation of IL-6 and CCL-2 gene expressions at 3 hours after stimulation (Figure 5A) because they were transcriptionally regulated by the NF-κB signaling pathway. Our results suggested that the reduction of these inflammatory mediators was indirectly regulated by downregulation of *Neat1* at the early time of LPS stimulation. However, we could not rule out that a long-term (12 hours and beyond) suppression of inflammatory responses may inhibit the NF-κB signaling pathway through the secondary effects. LncRNAs regulate gene expression at the levels of chromatin remodeling, transcription, and post-transcriptional processing.[36] *Neat1* can act as microRNA sponges[37] or transcription regulators using protein-binding partners[38,39] to activate or repress gene expression.[40] It remains unclear how *Neat1* regulates inflammation during AKI. Inflammasomes are

critical multiprotein complexes of the innate immune system that regulate caspase-dependent inflammation, cell death, and other cellular pathways.[41] Activation of the NLRP3 inflammasome triggers downstream inflammatory cytokines, with consequent cell apoptosis and ultimately AKI.[42] Our mechanistic studies indicated that *Neat1* promoted the assembly of NLRP3 inflammasome in part through interaction with Rack1 in LPS-stimulated tubular epithelial cells. Knockdown of *Neat1* reduced NLRP3 expression and caspase-1 activation, resulting in preserved kidney function in LPS-induced AKI mice. *In vitro*, knockdown of *Neat1* disrupted ASC oligomerization and protein–protein interaction between NLRP3 and ASC, suggesting a critical role of *Neat1* in regulating NLRP3 inflammasome assembly. Our findings on the role of *Neat1* in inflammasome activation were consistent with other studies.[43,44]

LncRNAs regulate biological functions by binding to DNA, RNAs (mRNAs and microRNAs), or proteins.[36,45] *Neat1* acts as a scaffold by interacting with RNA-binding proteins to enhance microRNA processing.[46] Interestingly, we found that *Neat1* bound to another scaffolding protein Rack1, which has previously reported as a critical mediator of NLRP3 inflammasome activation. Rack1, a multifunctional scaffold protein for kinases and receptors, mediates NLRP3 inflammasome activation in macrophages through direct binding to NLPR3, which promotes the active conformation of NLRP3 and inflammasome assembly.[47] Our results showed that *Neat1* knockdown disrupted the binding of Rack1 to NLRP3 upon stimulation with LPS plus nigericin, thereby inhibiting NLRP3 inflammasome assembly. Given that *Neat1* in tubular cells translocated from the nucleus into the cytoplasm after LPS plus nigericin stimulation (Supplemental Figure 7) and upon AKI (Supplemental Figure 8), it can be speculated that *Neat1* translocated to the cytoplasm where it binds the scaffold protein of Rack1 to regulate NLRP3 inflammasome assembly. In addition, the absence of either *Neat1* or Rack1 completely abrogated NLRP3 inflammasome activation in LPS-stimulated tubular epithelial cells, indicating the essential role of *Neat1* and Rack1 for NLRP3 inflammasome activation. Interestingly, overexpression of *Neat1*, but not Rack1 alone, activated NLPR3 inflammasome, suggesting an overarching role of *Neat1* in inflammasome complex formation. We also demonstrated that *Neat1* regulated NLRP3 inflammasome activation at the nuclear level. The induced expression of NLRP3 and IL-1β transcripts was inhibited in LPS-treated *Neat1*-deficient mice. *NEAT1* sequesters the protein splicing factor proline/glutamine-rich in paraspeckles, thereby enhancing the transcription of IL-8 from its promoter.[48] Future studies are warranted to elucidate the mechanism through which *Neat1* regulates the transcription of NLRP3 and IL-1β.

In conclusion, we have presented a spectrum of human, animal, and *in vitro* evidence for a novel role of lncRNA *Neat1* in AKI and unraveled its regulatory mechanisms toward NLRP3 inflammasome activation. In response to the septic stimulus from LPS, *Neat1* was upregulated in the kidney tubular compartment through the classical TLR4/NF-κB signaling pathway, and its interaction with Rack1 facilitates the inflammasome assembly to trigger inflammatory responses that orchestrate the subsequent phenotype characterized by tubular injury and loss of kidney function (Figure 8). *Neat1* is a prospective novel biomarker and therapeutic target for AKI.

Disclosures

Disclosure forms, as provided by each author, are available with the online version of the article at http://links.lww.com/JSN/E671.

Funding

This work was supported by the Research Grants Council of Hong Kong (Collaborative Research Fund, grant no. C7018-16G), Hong Kong Society of Nephrology/HK Kidney Foundation Research Grant 2019, and philanthropic donations from Dr. Rita T. Liu SBS of L & T Charitable Foundation Ltd. and Bingei Family of Indo Café, Mr. Winston Leung, Mr. K.K. Chan, and Ms. Siu Suet Lau. S.C.W. Tang is the awardee of an Endowment Fund established at the University of Hong Kong for the *Yu* Professorship in Nephrology. R. Xue received the HKU Postgraduate Fellowships in Integrative Medicine from 2018 to 2022. Publication was made possible in part by support from the HKU Libraries Open Access Author Fund sponsored by the HKU Libraries.

Acknowledgments

The funders played no role in the design or writing of this manuscript. Dr. Arthur Tang kindly assisted in extraction of clinical data of control participants in the cross-sectional AKI cohort study. Because Dr. Sydney C.W. Tang is an Associate Editor of *JASN*, he was not involved in the peer-review process for this manuscript. Another editor oversaw the peer-review and decision-making process for this manuscript.

Author Contributions

Conceptualization: Hui Yao Lan, Sydney C.W. Tang, Wai Han Yiu.
Data curation: Rui Xue.
Formal analysis: Kam Wa Chan, Rui Xue.
Funding acquisition: Kar Neng Lai, Sydney C.W. Tang.
Investigation: Rui Xue.
Methodology: Loretta Y.Y. Chan, Xiao Ru Huang, Hui Yao Lan, Hongyu Li, Sarah W.Y. Lok, Jingyuan Ma, Wai Han Yiu, Yixin Zou.
Project administration: Sydney C.W. Tang.
Supervision: Sydney C.W. Tang.
Writing – original draft: Rui Xue.
Writing – review & editing: Sydney C.W. Tang, Wai Han Yiu.

Data Sharing Statement

Anonymized data created for the study are or will be available in a persistent repository upon publication. Experimental Data. BioProject Accession. NA. The data has been deposited to the ProteomeXchange Consortium with the dataset identifier PXD048489.

Supplemental Material

This article contains the following supplemental material online at http://links.lww.com/JSN/E670.

Supplemental Figure 1. Kidney *Neat1* was successfully knocked down by the microbubble gene delivery technology.

Supplemental Figure 2. *NEAT1* expression in urinary sediment cells and buffy coat was significantly increased in patients with AKI.

Supplemental Figure 3. Knockdown of *Neat1* reduced circulating proinflammatory cytokine expression in LPS-induced, CLP-induced, and IR-induced AKI mice.

Supplemental Figure 4. Knockdown of *Neat1* attenuated macrophage infiltration in the kidney and suppressed tubular NLRP3 expression of LPS-induced, CLP-induced, and IR-induced AKI mice.

Supplemental Figure 5. Knockdown of *Neat1* protected against hypoxia-reoxygenation–induced inflammatory responses in mouse tubular C1.1 cells.

Supplemental Figure 6. Rack1 is a protein-binding partner of lncRNA *Neat1*.

Supplemental Figure 7. LPS/Nigericin induced *Neat1* translocation in mouse tubular C1.1 cells.

Supplemental Figure 8. Translocation of *Neat1* from the nucleus to the cytoplasm in the tubular cells of LPS-induced, CLP-induced, and IR-induced AKI mice.

Supplemental Table 1. Primers used in this study.

Supplemental Table 2. Etiologies of AKI in the study participants (N=66).

Supplemental Table 3. Association between AKI and urinary *NEAT1* expression.

Supplemental Table 4. Association between AKI and circulating (buffy coat) *NEAT1* expression.

References

1. Vijayan A. Tackling AKI: prevention, timing of dialysis and follow-up. *Nat Rev Nephrol.* 2021;17(2):87–88. doi:10.1038/s41581-020-00390-3
2. Chan KW, Yu KY, Lee PW, Lai KN, Tang SC. Global REnal involvement of CORonavirus disease 2019 (RECORD): a systematic review and meta-analysis of incidence, risk factors, and clinical outcomes. *Front Med (Lausanne).* 2021;8:678200. doi:10.3389/fmed.2021.678200
3. Peerapornratana S, Manrique-Caballero CL, Gomez H, Kellum JA. Acute kidney injury from sepsis: current concepts, epidemiology, pathophysiology, prevention and treatment. *Kidney Int.* 2019;96(5):1083–1099. doi:10.1016/j.kint.2019.05.026
4. Arshad A, Ayaz A, Rehman S, Ukrani RD, Akbar I, Jamil B. Progression of acute kidney injury to chronic kidney disease in sepsis survivors: 1-year follow-up study. *J Intensive Care Med.* 2021;36(11):1366–1370. doi:10.1177/0885066620956621
5. Ronco C, Bellomo R, Kellum JA. Acute kidney injury. *Lancet.* 2019;394(10212):1949–1964. doi:10.1016/S0140-6736(19)32563-2
6. Legrand M, Bell S, Forni L, et al. Pathophysiology of COVID-19-associated acute kidney injury. *Nat Rev Nephrol.* 2021;17(11):751–764. doi:10.1038/s41581-021-00452-0
7. Schmitt AM, Chang HY. Long noncoding RNAs in cancer pathways. *Cancer Cell.* 2016;29(4):452–463. doi:10.1016/j.ccell.2016.03.010
8. Kopp F, Mendell JT. Functional classification and experimental dissection of long noncoding RNAs. *Cell.* 2018;172(3):393–407. doi:10.1016/j.cell.2018.01.011
9. Yamazaki T, Souquere S, Chujo T, et al. Functional domains of NEAT1 architectural lncRNA induce paraspeckle assembly through phase separation. *Mol Cell.* 2018;70(6):1038–1053.e7. doi:10.1016/j.molcel.2018.05.019
10. Wang Y, Hu SB, Wang MR, et al. Genome-wide screening of NEAT1 regulators reveals cross-regulation between paraspeckles and mitochondria. *Nat Cell Biol.* 2018;20(10):1145–1158. doi:10.1038/s41556-018-0204-2
11. Wen S, Wei Y, Zen C, Xiong W, Niu Y, Zhao Y. Long non-coding RNA NEAT1 promotes bone metastasis of prostate cancer through N6-methyladenosine. *Mol Cancer.* 2020;19(1):171. doi:10.1186/s12943-020-01293-4
12. Yang YL, Xue M, Jia YJ, et al. Long noncoding RNA NEAT1 is involved in the protective effect of Klotho on renal tubular epithelial cells in diabetic kidney disease through the ERK1/2 signaling pathway. *Exp Mol Med.* 2020;52(2):266–280. doi:10.1038/s12276-020-0381-5
13. Zhang P, Cao L, Zhou R, Yang X, Wu M. The lncRNA Neat1 promotes activation of inflammasomes in macrophages. *Nat Commun.* 2019;10(1):1495. doi:10.1038/s41467-019-09482-6
14. Mangan MSJ, Olhava EJ, Roush WR, Seidel HM, Glick GD, Latz E. Targeting the NLRP3 inflammasome in inflammatory diseases. *Nat Rev Drug Discov.* 2018;17(8):588–606. doi:10.1038/nrd.2018.97
15. He Y, Hara H, Nunez G. Mechanism and regulation of NLRP3 inflammasome activation. *Trends Biochem Sci.* 2016;41(12):1012–1021. doi:10.1016/j.tibs.2016.09.002
16. Jo EK, Kim JK, Shin DM, Sasakawa C. Molecular mechanisms regulating NLRP3 inflammasome activation. *Cell Mol Immunol.* 2016;13(2):148–159. doi:10.1038/cmi.2015.95
17. Wang L, Hauenstein AV. The NLRP3 inflammasome: mechanism of action, role in disease and therapies. *Mol Aspects Med.* 2020;76:100889. doi:10.1016/j.mam.2020.100889
18. Elliott EI, Sutterwala FS. Initiation and perpetuation of NLRP3 inflammasome activation and assembly. *Immunol Rev.* 2015;265(1):35–52. doi:10.1111/imr.12286
19. Rathinam VAK, Zhao Y, Shao F. Innate immunity to intracellular LPS. *Nat Immunol.* 2019;20(5):527–533. doi:10.1038/s41590-019-0368-3
20. Wuthrich RP, Glimcher LH, Yui MA, Jevnikar AM, Dumas SE, Kelley VE. MHC class II, antigen presentation and tumor necrosis factor in renal tubular epithelial cells. *Kidney Int.* 1990;37(2):783–792. doi:10.1038/ki.1990.46
21. Pan LJ, Zhong TF, Tang RX, et al. Upregulation and clinicopathological significance of long non-coding NEAT1 RNA in NSCLC tissues. *Asian Pac J Cancer Prev.* 2015;16(7):2851–2855. doi:10.7314/apjcp.2015.16.7.2851
22. Wu Y, Yang L, Zhao J, et al. Nuclear-enriched abundant transcript 1 as a diagnostic and prognostic biomarker in colorectal cancer. *Mol Cancer.* 2015;14:191. doi:10.1186/s12943-015-0455-5
23. Chakravarty D, Sboner A, Nair SS, et al. The oestrogen receptor alpha-regulated lncRNA NEAT1 is a critical modulator of prostate cancer. *Nat Commun.* 2014;5:5383. doi:10.1038/ncomms6383
24. Bu FT, Wang A, Zhu Y, et al. LncRNA NEAT1: shedding light on mechanisms and opportunities in liver diseases. *Liver Int.* 2020;40(11):2612–2626. doi:10.1111/liv.14629
25. Wang Y, Hou L, Yuan X, et al. LncRNA NEAT1 targets fibroblast-like synoviocytes in rheumatoid arthritis via the miR-410-3p/YY1 Axis. *Front Immunol.* 2020;11:1975. doi:10.3389/fimmu.2020.01975
26. Gast M, Rauch BH, Haghikia A, et al. Long noncoding RNA NEAT1 modulates immune cell functions and is suppressed in early onset myocardial infarction patients. *Cardiovasc Res.* 2019;115(13):1886–1906. doi:10.1093/cvr/cvz085
27. Kinsey GR, Sharma R, Okusa MD. Regulatory T cells in AKI. *J Am Soc Nephrol.* 2013;24(11):1720–1726. doi:10.1681/ASN.2013050502
28. Linkermann A, Chen G, Dong G, Kunzendorf U, Krautwald S, Dong Z. Regulated cell death in AKI. *J Am Soc Nephrol.* 2014;25(12):2689–2701. doi:10.1681/ASN.2014030262
29. Kayagaki N, Wong MT, Stowe IB, et al. Noncanonical inflammasome activation by intracellular LPS independent of TLR4. *Science.* 2013;341(6151):1246–1249. doi:10.1126/science.1240248
30. Liu T, Zhang L, Joo D, Sun SC. NF-κB signaling in inflammation. *Signal Transduct Target Ther.* 2017;2:17023. doi:10.1038/sigtrans.2017.23
31. Lin M, Yiu WH, Wu HJ, et al. Toll-like receptor 4 promotes tubular inflammation in diabetic nephropathy. *J Am Soc Nephrol.* 2012;23(1):86–102. doi:10.1681/ASN.2010111210
32. Fu D, Ju Y, Zhu C, Pan Y, Zhang S. LncRNA NEAT1 promotes TLR4 expression to regulate lipopolysaccharide-induced trophoblastic cell pyroptosis as a molecular sponge of miR-302b-3p. *Mol Biotechnol.* 2022;64(6):670–680. doi:10.1007/s12033-021-00436-2
33. Nong W. Long non-coding RNA NEAT1/miR-193a-3p regulates LPS-induced apoptosis and inflammatory injury in WI-38 cells through TLR4/NF-κB signaling. *Am J Transl Res.* 2019;11(9):5944–5955. PMID: 31632562
34. Zhou W, Chen X, Hu Q, Chen X, Chen Y, Huang L. Galectin-3 activates TLR4/NF-κB signaling to promote lung adenocarcinoma cell proliferation through activating lncRNA-NEAT1 expression. *BMC Cancer.* 2018;18(1):580. doi:10.1186/s12885-018-4461-z

35. Zhou Y, Wang Y, Li Q, et al. Downregulation of lncRNA NEAT1 alleviates sepsis-induced acute kidney injury. *Cent Eur J Immunol.* 2022;47(1):8–19. doi:10.5114/ceji.2022.115628
36. Zhang X, Wang W, Zhu W, et al. Mechanisms and functions of long non-coding RNAs at multiple regulatory levels. *Int J Mol Sci.* 2019;20(22):5573. doi:10.3390/ijms20225573
37. Zhuang L, Xia W, Chen D, et al. Exosomal LncRNA-NEAT1 derived from MIF-treated mesenchymal stem cells protected against doxorubicin-induced cardiac senescence through sponging miR-221-3p. *J Nanobiotechnology.* 2020;18(1):157. doi:10.1186/s12951-020-00716-0
38. Chen Q, Cai J, Wang Q, et al. Long noncoding RNA *NEAT1*, regulated by the EGFR pathway, contributes to glioblastoma progression through the WNT/β-Catenin pathway by scaffolding EZH2. *Clin Cancer Res.* 2018;24(3):684–695. doi:10.1158/1078-0432.CCR-17-0605
39. Zhang M, Weng W, Zhang Q, et al. The lncRNA NEAT1 activates Wnt/β-catenin signaling and promotes colorectal cancer progression via interacting with DDX5. *J Hematol Oncol.* 2018;11(1):113. doi:10.1186/s13045-018-0656-7
40. Li W, Zhang Z, Liu X, et al. The FOXN3-NEAT1-SIN3A repressor complex promotes progression of hormonally responsive breast cancer. *J Clin Invest.* 2017;127(9):3421–3440. doi:10.1172/JCI94233
41. Komada T, Muruve DA. The role of inflammasomes in kidney disease. *Nat Rev Nephrol.* 2019;15(8):501–520. doi:10.1038/s41581-019-0158-z
42. Li N, Wang Y, Wang X, Sun N, Gong YH. Pathway network of pyroptosis and its potential inhibitors in acute kidney injury. *Pharmacol Res.* 2022;175:106033. doi:10.1016/j.phrs.2021.106033
43. Yao T, Song Y, Li S, Gu J, Yan X. Inhibition of lncRNA NEAT1 protects endothelial cells against hypoxia/reoxygenation-induced NLRP3 inflammasome activation by targeting the miR-204/BRCC3 axis. *Mol Med Rep.* 2022;25(1):32. doi:10.3892/mmr.2021.12548
44. Chai X, Liang Z, Zhang J, et al. Chlorogenic acid protects against myocardial ischemia-reperfusion injury in mice by inhibiting Lnc Neat1/NLRP3 inflammasome-mediated pyroptosis. *Sci Rep.* 2023;13(1):17803. doi:10.1038/s41598-023-45017-2
45. Wang KC, Chang HY. Molecular mechanisms of long noncoding RNAs. *Mol Cell.* 2011;43(6):904–914. doi:10.1016/j.molcel.2011.08.018
46. Jiang L, Shao C, Wu QJ, et al. NEAT1 scaffolds RNA-binding proteins and the Microprocessor to globally enhance pri-miRNA processing. *Nat Struct Mol Biol.* 2017;24(10):816–824. doi:10.1038/nsmb.3455
47. Duan Y, Zhang L, Angosto-Bazarra D, Pelegrin P, Nunez G, He Y. RACK1 mediates NLRP3 inflammasome activation by promoting NLRP3 active conformation and inflammasome assembly. *Cell Rep.* 2020;33(7):108405. doi:10.1016/j.celrep.2020.108405
48. Imamura K, Imamachi N, Akizuki G, et al. Long noncoding RNA NEAT1-dependent SFPQ relocation from promoter region to paraspeckle mediates IL8 expression upon immune stimuli. *Mol Cell.* 2014;53(3):393–406. doi:10.1016/j.molcel.2014.01.009